Energy Deposition Phenomena in Partially Transparent Solids

J. A. Nemes* and P. W. Randles*
U.S. Naval Research Laboratory, Washington, D.C.

The response of partially transparent materials subjected to rapid near-surface energy deposition is characterized by various phenomena including thermal degradation, polymer pyrolysis, and dynamic stress effects resulting in spallation failure. This paper addresses the role of each of these phenomena in the assessment of material degradation due to near-surface energy deposition. Analytical expressions are developed to determine the effect that energy intensity and pulse duration have on each of these phenomena for broad material categories. Approximate solutions are used to determine the dominant phenomena.

Introduction

THE response of materials subjected to radiant energy is a problem that has received considerable attention since the early 1960's. Determination of the resulting temperature distribution and the dynamic response of materials to pulsed radiant energy have both been of interest. Solutions to these problems can be used to determine conditions under which material degradation will occur. This degradation can result from either thermal or mechanical effects. Ultimately, the response is determined by the material properties, energy intensity, pulse duration, and spatial deposition profile. The response of materials to a uniform deposition profile was recently addressed by Nemes and Chang.[1] In the following, the response of partially transparent materials subjected to electromagnetic radiation, which is uniform at the exposed surface, will be considered. Materials that are partially transparent absorb energy near the front surface, resulting in a distribution that is nonuniform with depth. Since the primary interest here is in understanding the material response at the front surface of the material and consideration is given to the case where the depth of energy absorption is small in comparison to the material thickness, a half-space geometry is used in both the thermal and dynamic response solutions.

Following a discussion of the phenomena leading to material degradation, the general equations governing each of the phenomena are developed. Solutions are then obtained for the specific spatial and temporal distribution appropriate for a partially transparent material subjected to a pulsed energy source. The solutions are then used to identify regimes based on energy intensity and pulse duration in which each of the degradation phenomena is dominant. An example is given to illustrate how the regimes are defined.

Degradation Phenomenology

The degradation phenomena of partially transparent materials subjected to rapid energy deposition can be separated into those that are primarily thermal in nature and those in which mechanical effects dominate. The purely thermal phenomena include material degradation associated with elevated temperature and material removal or ablation. Ablation occurs under conditions in which sufficient energy is deposited to reach melt or sublimation. Because these thermal phenomena are dominant for materials subjected to continuous wave (cw) lasers, they have received considerable attention over the last twenty years. The authors and their colleagues at the Naval Research Laboratory[2–5] are among those who have studied the response of structural materials to the cw laser.

The understanding of phenomena caused by mechanical effects is not nearly as clear as those caused by thermal effects. Observation of mass particles being ejected when materials are subjected to short-pulse radiation has led to many different material models, with varying degrees of sophistication, to account for the presence of this discrete mass removal. Although these models have been somewhat successful in predicting overall material response, they are usually developed for a particular intensity and pulse duration. Thus, their applicability over a wide range of deposition parameters is questionable without a full understanding of the mechanics which leads to this observed phenomenon. Two separate mechanical effects that can lead to discrete mass removal are discussed.

The first of these mechanisms is postulated primarily for polymeric materials or composite materials with polymeric constituents. The mechanism, which was defined by Nienberg and Rubin,[6] is a result of heating due to direct energy deposition or through thermal conduction. Upon reaching sufficient temperatures, pyrolysis reactions take place, resulting in gaseous products in addition to a solid char residue. These pyrolysis gases, initially contained in existing voids, will be under increasing thermodynamic pressure, with either increasing temperature or increasing volume of gas. However, since the material is not impermeable, gas flow takes place within the material toward the free surface. If the rate of pressure increase exceeds the pressure relief from diffusion, large stresses develop within the material leading to possible fracture and resulting discrete mass removal.

The second mechanism that can lead to discrete particle removal is front-face spallation, which is a dynamic fracture that occurs under superposition of a relief or rarefraction wave from the free surface with the highly energized compressive stress state. There are several means by which rapid energy sources can produce waves in materials but this treatment is limited to waves produced by the rapid deposition of energy at the near surface, but over a finite thickness. It is important at this point to note that this discussion is aimed at front-face spallation. As is well known, the compressive waves generated by rapid energy deposition will traverse the thickness of the material and, upon encountering either a material of lower impedance or a free surface, be reflected as a tensile wave. This condition can lead to spallation of the rear surface, which also leads to failure or degradation of the structure. Since, however, rear-face spallation can be addressed outside the frame work of energy deposition phenomena, it will not be considered further.

The various phenomena discussed are shown schematically in Fig. 1. An understanding of the role that each of these phenomena has on material degradation can be gained by consideration of the one-dimensional heat conduction, pressure diffusion, and stress-wave equations. Such a one-dimensional treatment is equivalent to considering the energy flux to be uniform over the surface dimensions.

Received Oct. 20, 1987; revision received April 23, 1988.

*Mechanical Engineer, Mechanics of Materials Branch.

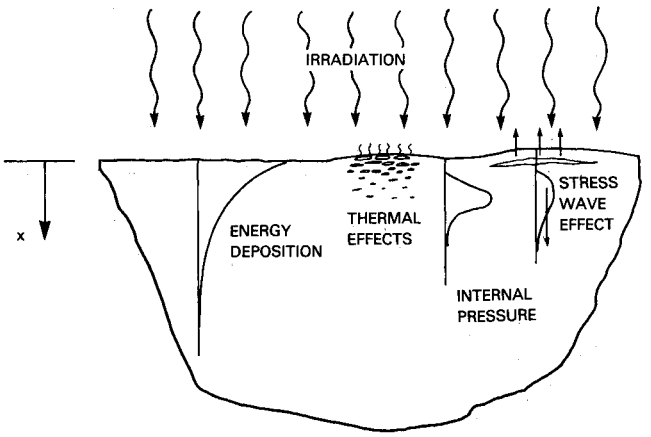

Fig. 1 Schematic of energy deposition effects.

Thermal Degradation

The response of material subjected to low-intensity continuous energy deposition or pulsed sources of long duration can be described in terms of thermal effects alone. Temperature distributions in the body can be obtained by considering the nonhomogeneous heat conduction equation, which follows:

$$\rho c \frac{\partial T}{\partial t} = \frac{\partial}{\partial x}\left[k_x \frac{\partial T}{\partial x}\right] + \rho Q(x,t) + \rho H \tag{1}$$

where

T = temperature	c = heat capacity
t = time	k_x = thermal conductivity
x = spatial variable	Q = energy deposition
ρ = density	H = heat of reaction

In general, the material property terms ρ, c, and k_x are functions of temperature. The heat of reaction term represents the heat that is absorbed during phase changes, including pyrolysis. Solutions to Eq. (1) for various boundary and initial conditions and for different forms of $Q(x,t)$ have been considered in studying material response to electromagnetic radiation. Reference 7 considers the problem of a half-space subjected to a step increase in temperature applied to the boundary, whereas Ref. 8 considers different forms for the volume energy deposition. The problem of a slab is treated in Refs. 9 and 10. A two-dimensional solution for a step increase in temperature at the surface is given in Ref. 11.

For materials that are partially transparent to radiation, the spatial variation of the volume energy deposition is assumed to be

$$Q(x,t) = Q_0(t)e^{-\alpha x} \tag{2}$$

where Q_0 is the surface energy deposition, and α is the inverse characteristic length.

The energy deposited per unit area is found by integrating Eq. (2) spatially and temporally. The characteristic length is considered to be constant during the energy deposition, but may be in fact a function of temperature or material state. Consideration of such a variable deposition introduces severe nonlinearities and is ignored in this development. Reference 12 considers temperature-varying deposition for continuous irradiation on a slab. For the partially transparent materials under consideration, the inverse characteristic length is such that the layer of substantial energy absorption can be taken to be finite. This is in contrast to opaque materials, such as metals, where α is such that the energy is considered to be deposited essentially at the surface, resulting in material response phenomena which are somewhat different than those presently being considered.

Pyrolysis-Induced Mass Removal

Many polymers, especially those that are of structural interest, including epoxies, phenolics, and polyimides, undergo pyrolysis reactions upon heating. Although the details of the chemical reactions that occur during pyrolysis are beyond the scope of this paper, the products of that reaction are of interest in the subsequent development. Simply, pyrolysis of these polymers yields both gaseous products and a solid char residue. Under conditions in which energy is deposited over an appreciable depth or where conduction has brought about increased temperature in depth, the pyrolysis reactions are thought to occur at voids within the material as well as at the surface. If the pyrolysis rate exceeds the rate in which the gases can be either stored or relieved through diffusion, then the resulting gas pressures can lead to material blowoff at the front surface.

The rate at which pyrolysis occurs is a function of both the reaction kinetics and the degree to which the reaction has progressed. The reaction rate can then be described by the following equation:

$$\frac{\partial \lambda}{\partial t} = -k\lambda^n \tag{3}$$

where k is the rate constant, n is the reaction order, and λ is a nondimensional density that denotes the mass fraction of unpyrolyzed material defined as

$$\lambda = (\rho - \rho_c)/(\rho_0 - \rho_c) \tag{4}$$

The subscripts o, c denote initial and fully charred densities, respectively. The rate constant can be defined by an Arrhenius equation given by

$$k = Ae^{-E_a/RT} \tag{5}$$

where A is the pre-exponential constant, E_a is the activation energy, and R is the gas constant.

Considering the conservation of mass for a fixed volume gives a relation between the average solid density ρ, the gas density in the pores ρ_g, and the net gas flow through the volume. The rate of change of solid density is $(\partial\rho/\partial t)$. The rate of change of gas density is $(\partial/\partial t)(\rho_g\varepsilon)$, and $(\partial/\partial x)(\rho_g v_g)$ is the gas flux through the volume. The balance expression yields the following:

$$-\frac{\partial \rho}{\partial t} = \frac{\partial}{\partial t}(\rho_g\varepsilon) + \frac{\partial}{\partial x}(\rho_g v_g) \tag{6}$$

where ρ_g is the gas density, v_g is the gas velocity, and ε is the void volume fraction.

The density of the gas can be related to the pressure and temperature by assuming local equilibrium and using the equation of state for an ideal gas given by

$$\rho_g = P/RT \tag{7}$$

In addition, the flow of gas through the porous material can be related to the pressure gradient by Darcy's law given as

$$v_g = -K/\mu \frac{\partial P}{\partial x} \tag{8}$$

where K is the permeability, and μ is the absolute viscosity. Using Eqs. (7) and (8), Eq. (6) can be written as

$$-\frac{\partial \rho}{\partial t} = \varepsilon \frac{\partial}{\partial t}\left[\frac{P}{RT}\right] + \left[\frac{P}{RT}\right]\frac{\partial \varepsilon}{\partial t} - \frac{\partial}{\partial x}\left[\frac{P}{RT}\frac{K}{\mu}\frac{\partial P}{\partial x}\right] \tag{9}$$

The following additional relationship between void volume and density change will be assumed.

$$\varepsilon = \varepsilon_0 + \frac{\rho_0 - \rho}{\rho_0}(1 - \varepsilon_0) \tag{10}$$

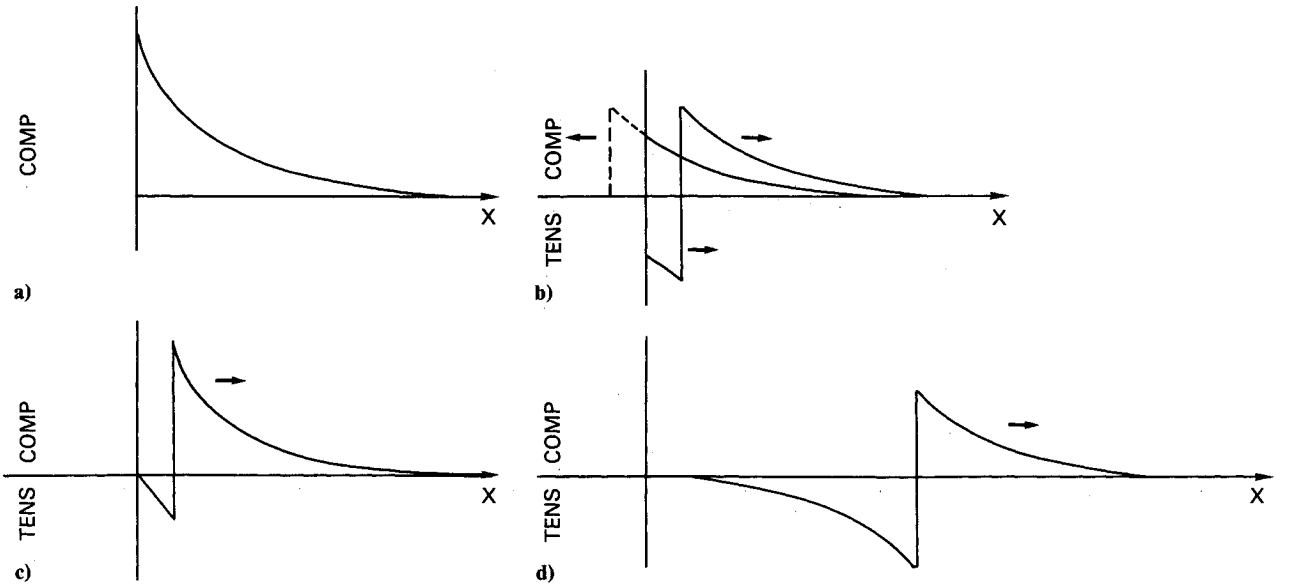

Fig. 2 Generation of stress waves from instantaneous energy deposition. Stress vs position is shown at successive instants of time.

It should be noted that Eq. (9) can be interpreted as a nonlinear diffusion equation for the pressure.

Front-Face Spallation

When energy deposition takes place at extremely rapid rates, dynamic effects in the material become significant. Stress waves generated in partially transparent material may lead to degradation or to complete separation of material in a type of failure termed spallation. When energy is deposited over some finite depth, stress waves are generated from the rapid heating of the material. The case of instantaneous deposition has been addressed by Morland,[13] Hegemier and Morland,[14] and Hegemier and Tzung.[15] Since the material is inertially confined, compressive stresses are generated within the material. Figure 2 illustrates the development of stress waves for the case of instantaneous deposition. So-called traveling waves, having an amplitude of one-half of the initial amplitude, are propagated in each direction, with those traveling to the left being reflected as tensile waves when they encounter the front face. Superposition of these waves shown in Fig. 2c leads to tensile stresses that, if of sufficient magnitude, can result in spallation. Only with finite spatial deposition will tensile stresses be produced.

The governing equations for the propagation of stress waves in the material are simplified to the one-dimensional momentum and energy balance expressions

$$\rho \frac{\partial^2 u}{\partial t^2} = \frac{\partial \sigma}{\partial x} \tag{11}$$

$$\rho \frac{\partial \xi}{\partial t} = \sigma \frac{\partial^2 u}{\partial x \partial t} + \frac{\partial h}{\partial x} + \rho Q(x,t) \tag{12}$$

where

u = particle displacement
σ = normal stress
ξ = internal energy density
h = heat flux

The individual terms of Eq. (12) correspond to the internal energy rate, strain energy rate, heat flux, and volumetric energy deposition rate, respectively. Equation (1), which is the heat conduction equation, is also an energy balance expression. It, however, neglects the strain energy and is written in terms of temperature instead of internal energy. Equations (11) and (12) are used in conjunction with the boundary condition

$$\sigma(0,t) = 0 \tag{13}$$

and an appropriate constitutive equation that is usually taken as an equation-of-state relationship.

Calculations

In this section, several solutions are presented to define the regimes in which each of the phenomena of interest (i.e., thermal degradation and material removal due to pyrolysis and stress-wave effects) are significant for the case in which the volumetric energy deposition in Eqs. (1) and (12) is given by

$$Q(x,t) = Q_0 e^{-\alpha x}[H(t) - H(t - t_0)] \tag{14}$$

where $H(t)$ is the Heaviside step function, and t_0 is the pulse length. Using the governing equations that have been presented in the preceding sections, expressions can be developed to determine material response through the use of some simplifying assumptions. Although the assumptions made would be overly restrictive for determination of accurate solutions to these problems for real materials, they do permit insight into an extremely complicated problem so that regimes for the various phenomena can be obtained and interactions between phenomena can be better understood.

Thermal Solution

A general solution to Eq. (1) can be obtained only through the use of numerical techniques, such as the finite-difference method. If however, it is desired to obtain an analytical solution to determine a threshold of thermal degradation, some simplifying assumptions can be made such that a closed-form solution is possible. First, since the solution is for onset of thermal damage, there will be no pyrolysis or sublimation so that the heat of reaction term in Eq. (1) can be neglected. Second, since the temperature changes will not be extreme, the variation of the material thermal properties with temperature will be negligible. With these assumptions, a solution to Eq. (1) can be obtained in conjunction with the initial and boundary conditions

$$T(x,0) = 0, \qquad \frac{\partial T}{\partial x}(0,t) = 0, \qquad \lim_{x \to \infty} T(x,t) = 0 \tag{15}$$

A Green's function method can be used, as done by Bechtel,[8] to obtain a solution in the form

$$T(x,t) = F(x,t) - F(x,t - t_0) \tag{16}$$

where

$$F(x,t) = (Q_0/c\alpha^2\kappa)H(t)\{-e^{-2X\Upsilon} + \tfrac{1}{2}e^{\Upsilon^2}[e^{2X\Upsilon}erfc(\Upsilon + X) + e^{-2X\Upsilon}erfc(\Upsilon - X)] + (2/\sqrt{\pi})\Upsilon e^{-X^2} - 2X\Upsilon erfc(X)\} \quad (17)$$

where $X = \frac{1}{2}(x/\sqrt{\kappa t})$, $\Upsilon = \alpha\sqrt{\kappa t}$, and $\kappa = k_x/\rho c$ is the thermal diffusivity.

In the limit where t_0 approaches zero, with the total energy flux $E = Q_0 t_0$ constant, the initial temperature distribution reduces to

$$T(x,0) = (E/\rho c)H(t)e^{-\alpha x} \quad (18)$$

as expected for instantaneous deposition.

Pyrolysis-Induced Degradation

The nonlinear nature of Eq. (9) and the coupling with the thermal solution makes an analytical solution extremely difficult. Thus, numerical techniques would be required to obtain a complete pressure history over the region. Equation (9) does, however, prove useful in determining a lower-bound solution of pyrolysis-induced degradation, that is, determination of the minimum energy to generate pyrolysis gases at rates sufficient to develop the internal pressures which lead to "blowoff."

Because the permeability is strongly dependent on porosity, permeabilities of unpyrolyzed material may be several orders of magnitude less than that of a fully charred material. Thus, determination of a lower-bound solution can be accomplished by allowing no gas flow out of the material. This reduces the mass conservation expression to a balance between the rate of decrease in solid mass and the rate of accumulation of gas in the voids.

$$-\frac{\partial \rho}{\partial t} = \frac{\partial}{\partial t}(\rho_g \varepsilon) \quad (19)$$

Using this equation in conjunction with Eq. (7) leads to the following development:

$$\frac{P}{RT}\varepsilon = -\int_0^t \frac{\partial \rho}{\partial t'}\,dt' = \rho_0 - \rho \quad (20)$$

From Eq. (4)

$$\frac{\partial \rho}{\partial t} = (\rho_0 - \rho_0)\frac{\partial \lambda}{\partial t} \quad (21)$$

Using Eqs. (3) and (5), this expression can be rewritten as

$$\frac{\partial \rho}{\partial t} = -Ae^{-E_a/RT}(\rho_0 - \rho_c)^{1-n}(\rho - \rho_c)^n \quad (22)$$

Integrating Eq. (22) yields

$$\rho = \rho_c + (\rho_0 - \rho_c)\left[1 - (1-n)A\int_0^t e^{-E_a/RT}\,dt'\right]^{\frac{1}{1-n}} \quad (23)$$

Using this result with Eq. (20) yields the following expression for pressure

$$P = \frac{RT}{\epsilon}(\rho_0 - \rho_c)\left\{1 - \left[1 - (1-n)A\int_0^t e^{-E_a/RT}\,dt\right]^{\frac{1}{1-n}}\right\} \quad (24)$$

For the case where $n = 1$, the result reduces to

$$P = \frac{RT}{\varepsilon}(\rho_0 - \rho_c)\left\{1 - \exp\left[-A\int_0^t e^{-E_a/RT}\,dt'\right]\right\} \quad (25)$$

Equation (24) or (25) can be solved numerically for the time-varying pressure within the voids corresponding to a given temperature history $T(x,t)$ at each position x. This pressure in turn can be used to approximate resulting tensile stresses in the material for determining conditions which lead to pyrolysis-induced degradation.

$$\sigma = P\varepsilon \quad (26)$$

Stress Waves

The governing equations for stress-wave generation caused by energy deposition over a finite depth were given as Eqs. (11–13). By considering small strains only, the strain energy rate on the right side of Eq. (12) can be neglected. Equation (12) can be further simplified by assuming negligible heat conduction effects over the times of interest. This assumption can be examined by comparing the change in temperature distribution over times comparable to wave travel times. This will be done for a specific material in a later section. Thus, the energy balance reduces to

$$\frac{\partial \xi}{\partial t} = Q \quad (27)$$

The solution of the problem posed by Eqs. (11), (13), and (27) requires specification of a constitutive relation. The following linear equation of state will be considered

$$\sigma = E_0\frac{\partial u}{\partial x} - \Gamma\rho\xi \quad (28)$$

where E_0 is the confined elastic modulus, and Γ is the Gruneisen ratio.

In general, both E_0 and Γ are functions of temperature. However, Hegemier and Tzung[15] showed that, whereas the wave form was affected by the variation of properties in the absorption layer, maximum tensile stresses were essentially independent of the distribution and depended only on the average value of Γ at $x = 0$ and the ratio of wave speeds $U(\infty)/U(0)$. Thus, Eq. (11) will provide a useful approximation for determining spallation thresholds. In accordance with Eq. (27), ξ is found by integrating Eq. (14), giving

$$\xi = Q_0 e^{-\alpha x}[tH(t) - (t - t_0)H(t - t_0)] \quad (29)$$

Then substituting Eq. (29) into Eq. (28), taking the spatial derivative, and then substituting the result into Eq. (11) yields the following:

$$\frac{\partial^2 u}{\partial t^2} = U_0^2\frac{\partial^2 u}{\partial x^2} + \alpha\Gamma Q_0 e^{-\alpha x}[tH(t) - (t - t_0)H(t - t_0)] \quad (30)$$

where $U_0 = \sqrt{E_0/\rho}$ is the wave velocity. Using the solution to Eq. (30) in conjunction with Eq. (28), an expression for stresses as a function of time and position is given by

$$\sigma(x,t) = (\Gamma\rho Q_0/\alpha U_0)\{\sinh[\alpha(U_0 t - x)]H(U_0 t - x) - \sinh[\alpha(U_0(t - t_0) - x)]H(U_0(t - t_0) - x) - e^{-\alpha x}\sinh(\alpha U_0 t)H(t) + e^{-\alpha x}\sinh[\alpha U_0(t - t_0)]H(t - t_0)\} \quad (31)$$

Using this expression, the effect of pulse length on maximum-developed tensile stress can be determined. Figure 3 shows the normalized tensile stress as a function of pulse length for different values of the material parameter αU_0. The term σ_{max} is equal to $\Gamma\rho Q_0 t_0$, which is the magnitude of the maximum compressive stress. Note that the maximum normalized stress, $|\sigma|/\sigma_{max} = 0.5$, which is indicated in Fig. 2 for instantaneous deposition.

Degradation Regimes

The results of the previous sections can be used to determine the onset of the degradation mechanisms that have been dis-

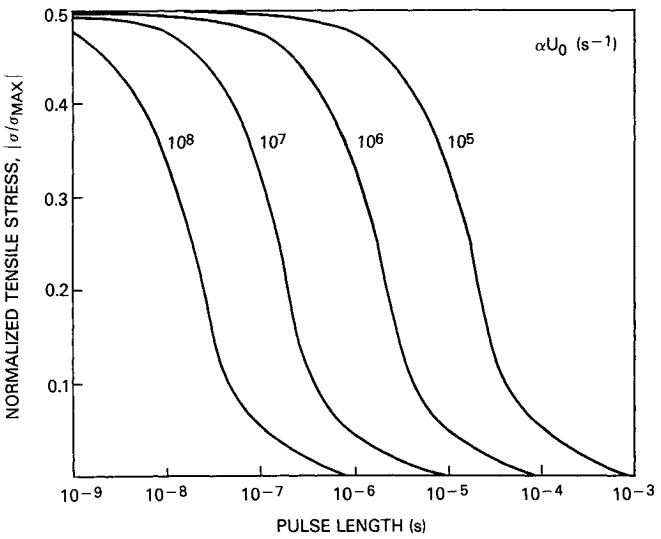

Fig. 3 Effect of pulse length on maximum tensile stress.

cussed thus far. In particular, it is of interest to determine the combination of energy intensity and pulse duration that leads to each phenomena. Intensity is expressed in terms of the surface energy deposition by the following:

$$I = \rho(Q_0/\alpha) \tag{32}$$

By considering limiting forms of the equations for temperature distribution, internal pressure, and dynamic stress, expressions can be developed to define these regimes.

The onset of thermal degradation is defined by a threshold temperature T_D. This temperature is usually taken as one in which significant reduction in strength would be expected or where residual degradation owing to pyrolysis would occur. Similarly, material sublimation is identified with conditions leading to an internal energy density which reaches the sublimation threshold ξ_s. Maximum temperature or internal energy occurs at the boundary $x = 0$ at the end of the pulse duration $t = t_0$. From Eqs. (16) and (17) this temperature is

$$T(0,t_0) = F(0,t_0) = (Q_0/c\alpha^2\kappa)[e^{\Upsilon_0^2}erfc(\Upsilon_0) + (2/\sqrt{\pi})\Upsilon_0 - 1] \tag{33}$$

where

$$\Upsilon_0 = \Upsilon|_{t=t_0} = \alpha\sqrt{\kappa t_0}$$

In terms of intensity, Eq. (33) can be rewritten as

$$I = \frac{\alpha k_x T(0,t_0)}{e^{\Upsilon_0^2}erfc(\Upsilon_0) + (2/\sqrt{\pi})\Upsilon_0 - 1} \tag{34}$$

where $k_x = \rho c\kappa$ has been used. By setting $T(0,t_0)$ equal to T_D, Eq. (34) can be used to determine the intensity that produces thermal degradation for a given pulse length. If $\Upsilon_0 \ll 1$, as in the case of very short pulses, Eq. (34) can be approximated by

$$I \cong \frac{\alpha k_x T(0,t_0)}{\Upsilon_0^2} = \frac{\rho c T(0,t_0)}{\alpha t_0} \tag{35}$$

which is a constant absorbed-energy curve, $It_0 = \text{constant}$.

Material blowoff because of pyrolysis is bounded by considering no gas flow, so that the internal pressure is given by Eqs. (24) or (25). Gas flow reduces the internal pressure and subsequently the tensile stress on the solid material. With no gas flow, the maximum pressure occurs at the surface where the temperature, given by Eq. (16), is also a maximum. Resulting tensile stresses can then be compared using Eq. (26) and compared with a maximum tensile stress to determine conditions leading to pyrolysis-induced blowoff.

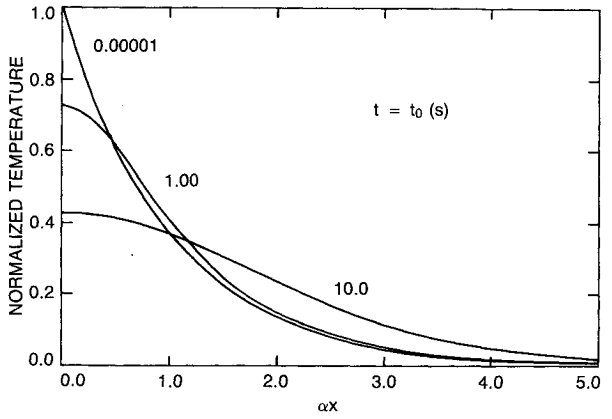

Fig. 4 Temperature distribution at various pulse lengths.

Table 1 Material parameters

$\alpha = 10.0$ cm^{-1}	$R = 0.693$ J/g
$\rho_0 = 1.25$ g/cm^3	$\rho_c = 0.180$ g/cm^3
$\kappa = 0.001$ cm^2/s	$E_a = 1.35 \times 10^4$ J/g
$k_x = 0.00235$ W/cm C	$\sigma_s = 10$ MPa
$A = 1.35 \times 10^{10}$ s^{-1}	$\Gamma = 0.20$
$n = 1$	$U_0 = 2 \times 10^5$ cm/s
$\varepsilon_0 = 0.05$	$T_D = 350$ C
	$\xi_s = 60000$ J/g

The onset of front-face spallation is determined from the maximum tensile stress predicted by Eq. (31). Stresses are a maximum along the characteristic, $x = U_0(t - t_0)$. The corresponding stress is

$$\sigma|_{x=U_0(t-t_0)} = (\Gamma\rho Q_0/2\alpha U_0)(1 - e^{-\alpha U_0 t_0})(1 - e^{-2\alpha x}) \tag{36}$$

Since an elastic material is considered in this solution, no dispersion or dissipation takes place, leading to maximum stresses as $x \to \infty$. Using this as a bounding estimate, the maximum tensile stress σ_{tens} is given by

$$\sigma_{\text{tens}} = (\Gamma\rho_0 Q_0/2\alpha U_0)(1 - e^{-\alpha U_0 t_0}) \tag{37}$$

Setting this maximum stress equal to a spallation stress σ_s, and rewriting Eq. (37) in terms of intensity, gives the following relation for the intensity required to cause spallation for a given pulse length.

$$I = [2U_0\sigma_s/\Gamma(1 - e^{-\alpha U_0 t_0})] \tag{38}$$

If $\alpha U_0 t_0 \ll 1$, as for the case of very short pulses, then

$$I \cong 2\sigma_s/\Gamma\alpha t_0 \tag{39}$$

which is another constant absorbed-energy curve. If $\alpha U_0 t_0 \gg 1$ as for very long pulses, but which are abruptly shut off, then

$$I \cong 2\sigma_s U_0/\Gamma \tag{40}$$

Example

To illustrate the use of the preceding equations, a specific example is presented. The material parameters considered are shown in Table 1. Although the parameters are primarily used for the example, they are representative of those found for a porous epoxy. Using these parameters, several important points made during the development can be illustrated.

First, using Eqs. (16) and (17), the temperature distribution at $t = t_0$ is computed for several different pulse lengths and is shown in Fig. 4. As can be seen in the figure, the temperature distribution at times $t = 1.0 \times 10^{-5}$ and $t = 1.0$ s are not tremendously different. The effects of heat conduction there-

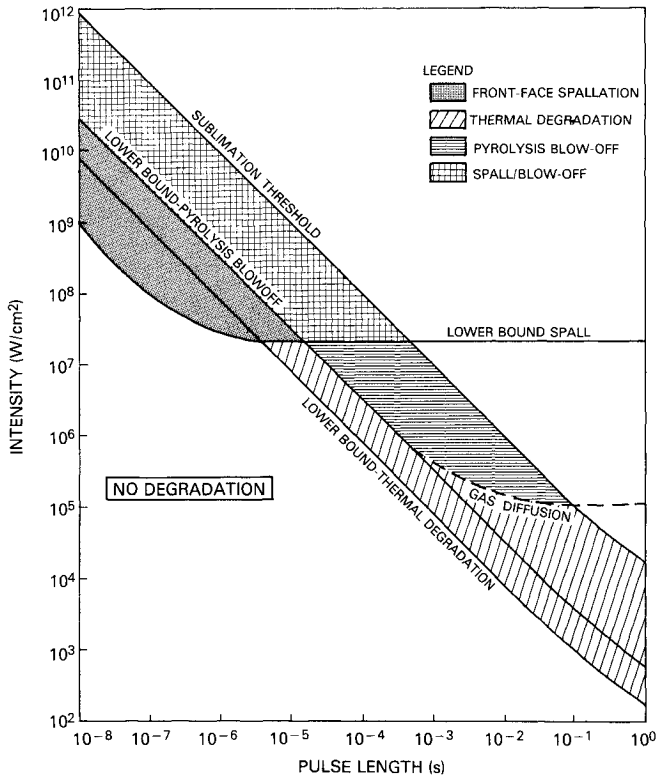

Fig. 5 Material-response diagram.

fore are important only for long pulse duration. In addition, since wave travel times are $\ll 1.0$ s, the neglection of heat flux in the energy balance expression, Eq. (12), is certainly justified.

Secondly, the parameter αU_0 for the example material is $2.0 \times 10^6\ s^{-1}$. From Fig. 3, the importance of considering the pulse to be finite rather than instantaneous becomes apparent for pulse durations greater than 10^{-7} s for this value of αU_0. At these longer pulse lengths, normalized tensile stresses become significantly less than the instantaneous value of 0.5.

Finally, using the expressions developed in the previous section and the parameters from Table 1, bounds for thermal degradation, sublimation threshold, pyrolysis-induced blowoff, and front-face spallation are plotted on a material response diagram, as shown in Fig. 5. The diagram is developed in terms of absorbed intensity vs pulse length. The dashed line in the figure, defined as gas diffusion, represents only an indication of the effect that retention of the gas flow term in Eq. (6) would have on the pyrolysis blowoff region. The bounds developed for each of the phenomena then define regimes in intensity pulse-length space, where phenomena would be expected to dominate. The regimes are also indicated in Fig. 5.

Concerning the regimes themselves, it should be noted first that the region above the sublimation line has not been considered in the scope of this paper, but obviously would be one in which a combination of phenomena could be expected. Multiple phenomena could also be expected in the region defined as Spall/Blowoff. In this region it may be possible to determine dominant phenomena by considering the location and sequence of events which would be expected to occur. For instance, spallation does not occur until after the pulse is shut off. Thus, if sufficient gas pressure is developed before the end of the pulse, blowoff would occur. Conversely, spallation would occur if the time to develop sufficient gas pressure exceeds the pulse length plus wave transit time. Additional insight can be gained by examining the two phenomena spatially, that is, the depth to which blowoff would occur in comparison to the potential spall plane. Examination of Eq. (36) shows that the depth of spall decreases with increasing intensity. However, at sufficient intensities the material will exhibit multiple spallation, a topic that has not been addressed in this paper. Thus, regions of multiple phenomena are extremely complex and will certainly require further study.

Conclusions

This paper has examined the role of front-face spallation, pyrolysis blowoff, and thermal effects in the degradation of material subjected to pulsed energy sources. The governing equations for each of these phenomena have been presented. Expressions have been developed to determine both temperature and stress distributions in a half-space subjected to energy deposition of a finite pulse duration. Using these expressions, a material-response diagram has been developed, which shows the dominant phenomena as a function of absorbed intensity and pulse duration. Using the results obtained in this paper, several conclusions can be reached.

1) Thermal diffusion and stress-wave effects are well separated in relation to pulse duration and therefore have negligible interaction on a macroscopic scale. Interaction of effects on a local scale in heterogeneous material has yet to be investigated.

2) Materials subjected to very short pulsed radiation may exhibit stress wave, pyrolysis blowoff, and thermal effects. For intermediate pulse lengths, pyrolysis blowoff and thermal effects may be present, with only thermal effects being apparent for long pulse durations.

3) Front-face spallation may occur without significant thermal degradation or pyrolysis for short pulse duration and high intensities.

Although the conclusions reached are important for the insight gained to understanding the problem of material response to rapid energy sources, the need for further work in this area is apparent. Several topics for future study would include:

1) Investigation of synergistic effects between phenomena, especially in the regions of pulse duration—intensity space where front-face spallation and pyrolysis blowoff overlap.

2) Evaluation of material nonlinearities and attenuating mechanisms in stress-wave generation and evaluation of temperature-dependent properties and phase changes in thermal distribution.

3) Understanding of the characteristic length and consideration of nonlinear characteristic lengths.

4) The effects of material heterogeneity.

References

[1]Nemes, J. A. and Chang, C. I., "Structural Response of Materials Due to In-Depth Heating," *Journal of Thermophysics and Heat Transfer*, Vol. 1, July 1987, pp. 201–208.

[2]Griffis, C. A., Masumura, R. A., and Chang, C. I., "Thermal Response of Graphite Epoxy Composite Subject to Rapid Heating," *Journal of Composite Materials*, Vol. 19, Sept. 1985, pp. 427–442.

[3]Griffis, C. A., Nemes, J. A., Stonesifer, F. R., and Chang, C. I., "Degradation in Strength of Laminated Composites Subjected to Intense Heating and Mechanical Loading," *Journal of Composite Materials*, Vol. 20, May 1986, pp. 216–235.

[4]Griffis, C. A., Chang, C. I., and Stonesifer, F. R., "Thermomechanical Response of Tension Panels Under Intense Rapid Heating," *Theoretical and Applied Fracture Mechanics*, Vol. 3, March 1985, pp. 41–48.

[5]Chang, C. I., Griffis, C. A., Stonesifer, F. R., and Nemes, J. A., "Thermomechanical Effects of Intense Heating on Materials/Structures," *Journal of Thermophysics and Heat Transfer*, Vol. 1, April 1987, pp. 175–181.

[6]Nienberg, J. W. and Rubin, I., "Analysis of Booster Materials Response to Repetitively Pulsed Laser Radiation," *Proceedings of the AIAA Laser Effects and Target Response Meeting*, DNA 001-85-C-0309, Washington, DC, Dec. 1985, pp. 243–254.

[7]Boley, B. A. and Tolins, I. S., "Transient Coupled Thermoelastic Boundary Value Problems in the Half-Space," *Journal of Applied Mechanics*, Vol. 29, Dec. 1962, pp. 637–646.

[8]Bechtel, J. H., "Heating of Solid Targets with Laser Pulses," *Journal of Applied Physics*, Vol. 46, April 1975, pp. 1585–1593.

[9]Danilovskaya, V. I. and Zubchaninova, V. N., "Temperature Fields and Stresses Created in a Plate by Radiant Energy," *Prikladnaya Mekhanika*, Vol. 4, Jan. 1968, pp. 103–110.

[10]Paramasivam, T. and Reismann, H., "Laser-Induced Thickness

Stretch Motion of a Transversely Constrained Irradiated Slab," *AIAA Journal*, Vol. 24, Oct. 1986, pp. 1650–1655.

[11]Jaunzemis, W. and Sternberg, E., "Transient Thermal Stresses in a Semi-Infinite Slab," *Journal of Applied Mechanics*, March 1960, pp. 93–103.

[12]Liarokapis, E. and Raptis, Y. S., "Temperature Rise Induced by a CW Laser Beam Revisited," *Journal of Applied Physics*, Vol. 57, June 1985, pp. 5123–5126.

[13]Morland, L. W., "Generation of Thermoelastic Stress Waves by Impulsive Electromagnetic Radiation," *AIAA Journal*, Vol. 6, June 1968, pp. 1063–1066.

[14]Hegemier, G. A. and Morland, L. W., "Stress Waves in a Temperature-Dependent Viscoelastic Half-Space Subjected to Impulsive Electromagnetic Radiation," *AIAA Journal*, Vol. 7, Jan. 1969, pp. 35–41.

[15]Hegemier, G. A. and Tzung, F., "Stress-Wave Generation in a Temperature-Dependent Absorbing Solid by Impulsive Electromagnetic Radiation," *Journal of Applied Mechanics*, Vol. 37, June 1970, pp. 339–344.